Inverse-Designed Edge Couplers for Multimode Silicon Nitride Photonics

Julian L. Pita Ruiz[1,3,*], Samuel Gougeon[2,3], Mostafa Youssef[1,3], Bora Ung[1,3], Sophie LaRochelle[2,3], and Michaël Ménard[1,3]

[1]*Department of Electrical Engineering, École de Technologie Supérieure, Montréal QC H3C 1K3, Canada*
[2]*Electrical and Computer Engineering, Université Laval, Québec QC G1V 0A6, Canada*
[3]*Centre d'optique photonique et lasers, Université Laval, Québec QC G1V 0A6, Canada*
julian-leonel.pita-ruiz@etsmtl.ca

Abstract: We demonstrate inverse-designed five- and ten-mode edge couplers in silicon nitride for efficient coupling to elliptical-core fibers. They achieve coupling efficiencies of up to −2.4 dB and 3-dB bandwidths spanning the C and L bands. © 2026 The Author(s)

Fiber-to-chip couplers are critical building blocks in silicon photonics, underpinning applications ranging from data interconnects and sensing to LiDAR and quantum computing [1]. While extensive research has matured single-mode couplers to high performance, their multimode counterparts have seen comparatively little development [2]. This disparity is not due to a lack of applications but stems from the fundamental challenge of efficiently coupling multimode fibers to photonic integrated circuits without resorting to costly or non-commercial fabrication processes. As a result, integrated photonics has remained inaccessible for systems where multimode operation is essential–such as coherent LiDAR [3] or optical coherence tomography sensors, where the detection of reflected or distorted wavefronts provides intrinsic resistance to speckle noise. Furthermore, in space-division multiplexing datacom interconnects, overall capacity could be scaled by the number of supported modes [4], without requiring new modulator or laser architectures.

Silicon nitride has proven to be an excellent platform for realizing compact freeform, low-loss photonic devices [5]. In this study, we demonstrate two unprecedented freeform silicon nitride couplers designed for direct edge coupling to a highly elliptical-core fiber (HECF) for multimode applications. Both couplers have a compact footprint of 36 µm×40 µm. The first device supports coupling to five TE modes, while the second enables coupling to ten modes, encompassing both TE and TM polarizations. For the five-mode coupler, simulated efficiencies range from −1.5 dB to −2.5 dB, with measured values between −2.4 dB and −5.1 dB. The ten-mode coupler exhibits a peak simulated efficiency of −1.1 dB for the TM_{00}, TE_{01}, and TM_{01} modes, while the worst-case simulated efficiency of −2.1 dB occurs for the TE_{04} mode. Measured intensity profiles of the ten-mode coupler show strong mode fidelity with the targeted HECF modes. These results represent a significant improvement over existing state-of-the-art approaches, such as silicon multimode grating couplers [6]–which typically suffer from insertion losses exceeding 5.0 dB and require the combination of two or more inputs to generate a single fiber mode–or Ge-doped silica transition chips [7], which are limited to six modes and act as intermediate coupling interfaces, thereby increasing cost, footprint, and alignment complexity. Neither technology scales effectively to higher mode counts.

Figure 1 shows from left to right: the ten target modes of the HECF, a schematic of the coupling system, and

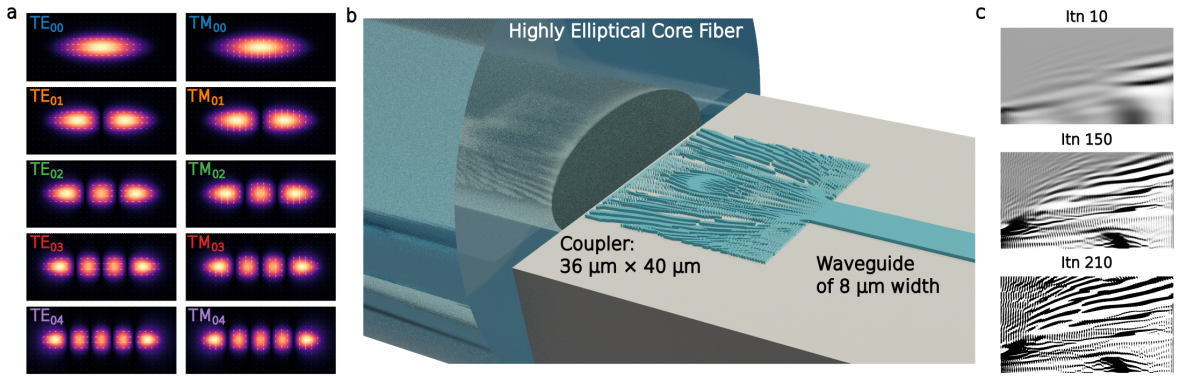


Fig. 1: **Inverse design of edge multimode couplers.** (a) Simulated field profiles of all modes supported by the highly elliptical-core fiber (HECF). (b) Schematic of the multimode coupling system showing the HECF aligned with the ten-mode coupler. (c) Three exemplary intermediate geometries of the ten-mode coupler, each taken from one of the three main stages of the optimization process: grayscale optimization, binarization, and design-for-manufacturing.

This Article © 2026 The Author(s)

three intermediate coupler geometries obtained during the design process. The polarization-maintaining HECF was optimized to support five spatial modes, each with two orthogonal polarizations (ten channels in total), and exhibits a modal birefringence greater than 10^{-4} for all guided modes [8]. The schematic shows [in Fig. 1(b)] the coupling configuration, where the HECF is aligned with the ten-mode coupler (top cladding removed for visualization). The couplers were fabricated on a 400 nm silicon nitride platform with a 4.5 µm bottom oxide and a 3 µm top cladding. The design was performed using LumOpt, a Python-based wrapper that employs gradient-based algorithms from SciPy to perform topology optimization. During the optimization process, a minimum feature constraint of 120 nm was imposed to ensure device fabricability.

Figure 2 presents the performance of the five-mode coupler. As shown in the simulated efficiency plot of Fig. 2(a), the devices exhibit a flat simulated efficiency across the target design band. The couplers were fabricated by Applied Nanotools (ANT) via an MPW run using electron-beam lithography and reactive ion etching. Figure 2(c) demonstrates that the freeform structure was successfully realized with no obvious geometric deviations. However, Fig. 2(d) indicates that for the TE_{04} mode, the central lobe is nearly absent, suggesting that fabrication variations may affect the performance of this specific mode more significantly than others. Figure 2(f) confirms that the absence of the central lobe reduces the measured efficiency from −2.8 dB predicted in simulation [Fig. 2(b)] to −5.5 dB at 1560.5 nm. For the other modes, measured efficiency remains in good agreement with simulations, ranging from −2.4 dB to −3.8 dB compared to the predicted −1.9 dB to −2.8 dB at 1560.5 nm.

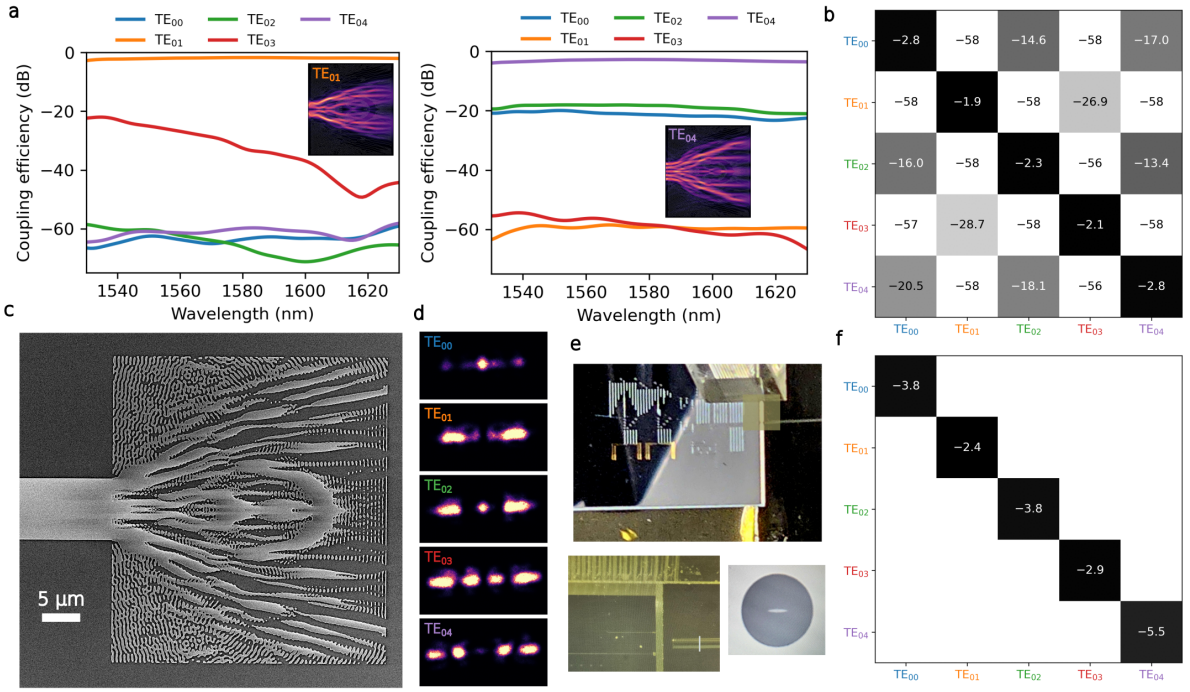


Fig. 2: **Five-mode coupler performance.** (a) Simulated coupling efficiency of the TE_{01} and TE_{04} modes across the full C and L bands, with an inset showing the top view of the electric field magnitude for both modes. (b) Matrix showing the simulated efficiency at 1560.5 nm of all modes when excited individually. (c) SEM image of the five-mode coupler. (d) Measured intensity profile at the edge of the chip for each excited mode. (e) Device under test, showing the fiber array used to feed each mode and the HECF during the alignment process. Insets show a close-up view of the chip edge and a cross-section image of the HECF. (f) Matrix showing the measured coupling efficiency at 1560.5 nm.

Figure 3 presents the performance of the ten-mode coupler. Figure 3(a) illustrates how effectively the freeform coupler expands the mode size to match that of the fiber modes, with each lobe enhanced as it propagates through the coupler. The simulated efficiency of the TM_{01} and TE_{04} modes exhibits a flat response across the full simulated range, similar to the five-mode coupler, highlighting the broadband capability of the device. Modal crosstalk is higher for modes with the same parity and increases at longer wavelengths. For instance, the TE_{04} mode, which shows the lowest performance among all modes, exhibits the highest crosstalk with the TE_{00} and TE_{02} modes, but it remains below −15.0 dB for most of the simulated range. The matrix in Fig. 3(c) illustrates this modal crosstalk trend and shows that the simulated coupling efficiency ranges from −1.1 dB to −2.1 dB at 1550.8 nm for all modes, indicating better performance than the five-mode coupler. A SEM image of the ten-mode coupler is shown in Fig. 3(d). For this device, a deep learning-based prefab model [9] was employed to compensate for fabrication variations during the ANT silicon nitride process. The measured intensity profiles at the chip edge,

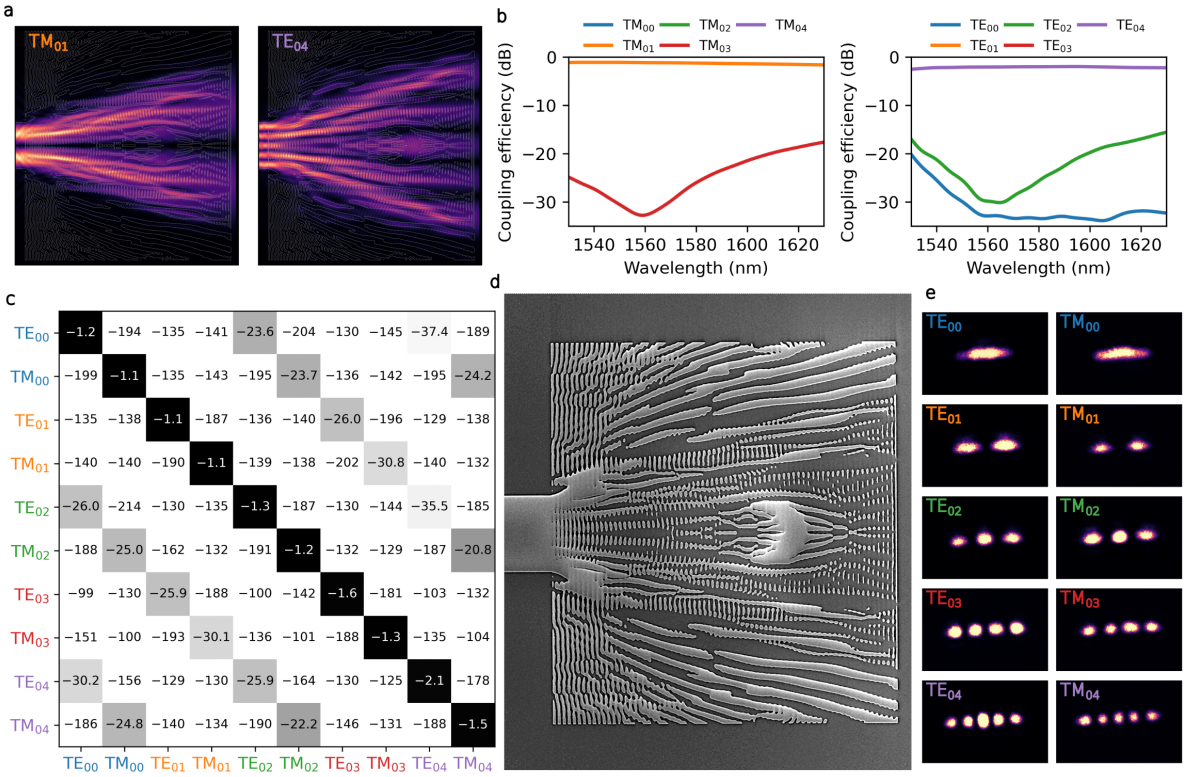


Fig. 3: **Ten-mode coupler performance.** (a) Top view of the electric field magnitude for the TM_{01} and TE_{04} modes. (b) Simulated efficiency of the TM_{01} to TE_{04} modes across the full C and L bands. (c) Matrix showing the simulated efficiency of all modes at 1550.8 nm when excited individually. (d) SEM image of the ten-mode coupler. (e) Measured intensity profile at the edge of the chip for each excited mode.

shown in Fig. 3(e), demonstrate good agreement with the HECF modes and predict high coupling efficiency. These profiles also exhibit improved mode fidelity compared to those of the five-mode coupler.

In conclusion, we have successfully demonstrated two unprecedented freeform silicon nitride multimode couplers with minimum feature sizes compatible with DUV fabrication, enabling efficient coupling to HECFs. These devices exhibit broadband performance, low insertion loss, and high mode fidelity, demonstrating their potential for scalable multimode photonic systems.

Funding. This research was funded by the Natural Sciences and Engineering Research Council of Canada (NSERC), by the Fonds de recherche du Québec (doi.org/10.69777/340950), and fabrication of the prototypes was supported by CMC Microsystems.

References

1. S. Shekhar, W. Bogaerts, L. Chrostowski, J. E. Bowers, M. Hochberg, R. Soref, and B. J. Shastri, "Roadmapping the next generation of silicon photonics," Nat. Commun. **15**, 751 (2024).
2. R. Marchetti, C. Lacava, L. Carroll, K. Gradkowski, and P. Minzioni, "Coupling strategies for silicon photonics integrated chips," Photonics Res. **7**, 201–239 (2019).
3. J.-D. Chen, W.-C. Miao, Y.-H. Hong, and H.-C. Kuo, "Recent advances in light detection and ranging: optical modulation solutions and novel nanotechnologies," Adv. Quantum Technol. **7**, 2300157 (2024).
4. K. Y. Yang, C. Shirpurkar, A. D. White, J. Zang, L. Chang, F. Ashtiani, M. A. Guidry, D. M. Lukin, S. V. Pericherla, J. Yang *et al.*, "Multi-dimensional data transmission using inverse-designed silicon photonics and microcombs," Nat. Commun. **13**, 7862 (2022).
5. J. L. Pita Ruiz, N. Dalvand, and M. Ménard, "Integrated silicon nitride devices via inverse design," Nat. Commun. **16**, 9307 (2025).
6. K. Lu, Z. Chen, H. Chen, W. Zhou, Z. Zhang, H. K. Tsang, and Y. Tong, "Empowering high-dimensional optical fiber communications with integrated photonic processors," Nat. Commun. **15**, 3515 (2024).
7. X. Yi, W. Zhao, L. Zhang, Y. Shi, and D. Dai, "Efficient mode coupling/(de) multiplexing between a few-mode fiber and a silicon photonic chip," Photonics Res. **12**, 2784–2793 (2024).
8. A. Corsi, J. Ho Chang, R. Wang, L. Wang, L. Ann Rusch, and S. LaRochelle, "Highly elliptical core fiber with stress-induced birefringence for mode multiplexing," Opt. letters **45**, 2822–2825 (2020).
9. D. Gostimirovic, Y. Grinberg, D.-X. Xu, and O. Liboiron-Ladouceur, "Improving fabrication fidelity of integrated nanophotonic devices using deep learning," ACS Photonics **10**, 1953–1961 (2023).